



ISSN: 0067-2904

Longitudinal Form Factors and Quadrupole Moments of $^{22,26}\text{Na}$ Isotopes with Different Interactions

Sh. K. Raheem, Z. A. Dakhil*

Department of Physics, College of Science, University of Baghdad, Baghdad, IRAQ

Received: 5/2/2022

Accepted: 4/4/2022

Published: 30/12/2022

Abstract

The longitudinal electron scattering form factors and the electric quadrupole moments are calculated for the states with $J^\pi T = 3^+0$ (ground state) and 1^+0 (583keV excited state) of ^{22}Na and $J^\pi T = 3^+2$ (ground state) of ^{26}Na . Shell model calculations are based on USDA, USDB and Wildenthal interactions. The exact center of mass correction is included in Born approximation picture to generate the longitudinal form factors. The core polarization (CP) effect with the values of effective nucleon charges $e_p=1.35$, $e_n=0.35$, with Bohr Mottelson formula gave a good agreement with the measured electric quadrupole moments. The structure of the nuclei under consideration shows that the $1d_{5/2}$ orbit is dominant configuration for ^{22}Na , and $2s_{1/2}$ orbit for ^{26}Na .

Keywords: Exotic nucleus, longitudinal electron scattering, quadrupole moment, *psd*-shell model

عوامل التشكل الطولية والعزوم رباعية القطب لنظائر الصوديوم $^{22,26}\text{Na}$ ولتفاعلات مختلفة

شهد كمال رحيم، زاهدة أحمد دخيل*

قسم الفيزياء، كلية العلوم، جامعة بغداد، بغداد - العراق

الخلاصة

تم حساب عوامل التشكل الطولية والعزوم رباعية القطب للحالات الموصوفة بـ $J^\pi T = 3^+0$ (الحالة الأرضية) و 1^+0 (583keV) للنواة ^{22}Na و 3^+2 (الحالة الأرضية) للنواة ^{26}Na . حسابات نموذج الأغلفة النووي استندت على التفاعلات USDA, USDB, W. تم إدخال القيمة المضبوطة لتصحیح حركة مركز الكتلة بصورة تقريب بورن لتعديل عوامل التشكل الطولية. ادخال تأثير استقطاب القلب لقيم الشحنة الفعالة للنيوكليون $e_p=1.35$, $e_n=0.35$ ومن صيغة بور موتلسن أعطى توافق جيد للنتائج الحالية مع القيم العملية لعزوم رباعية القطب. تركيب النوى قيد الدراسة بينت بان المدار $1d_{5/2}$ هو التوزيع المهيمن للنواة ^{22}Na , والمدار $2s_{1/2}$ للنواة ^{26}Na .

Introduction

Investigation of the properties of exotic nuclei becomes one of the most important goals in nuclear physics. Exotic feature in nuclear physics is of tremendous interest not only because it serves as a rigorous test for existing nuclear models, but also because it opens up

*Email: zahida.a@sc.uobaghdad.edu.iq

new study fields in nuclear science [1]. The shell model becomes more relevant in the exotica region of the nuclear chart, where predictive power is more required than in the stable nuclei region. The quadrupole (Q) moment can be considered as a unique tool to determine the deformation and collective behavior of nuclei both at low and high excitation energy [2]. Many studies have been carried out on the nuclear structure of stable and exotic nuclei through electron scattering. Keim et al. [3] measured the Q moments of $^{26-29}\text{Na}$ by β -NMR spectroscopy. Most quadrupole moments of nuclear ground states were obtained from measurements of the hyperfine structure of atomic energy levels. However, the quadrupole moments and even more the atomic hyperfine fields decrease with the atomic charge number Z . The exact value of the center of mass correction in the translation invariant shell model (TISM) had been included in previous work [4], in studying the longitudinal electron scattering form factors for the low lying excited states of ^7Li , and gave good results. The data are well described when the core polarization effects are included through effective nucleon charge.

Roca-Maza et al. [5, 6] studied the development of the charge form factors with proton and neutron numbers in different mass regions of the nuclear chart. They concluded that the elastic scattering of electron experiments in isotones can provide priceless information about occupation of the single-particle levels of protons and the filling order. The quadrupole moment data of exotic nuclei provide a qualitative directory to the structure of associated nuclear states. The effective charges and the quadrupole moments for Li and B isotopes have been calculated by Radhi et al. [7]. Their calculations were based on the shell model with p and large basis $spsdpf$ - shell model spaces. A microscopic theory was adopted in their calculations, which allowed particle-hole excitations from the core and model space orbits to all higher orbits with $6\hbar\omega$ excitations. The calculated effective charges for the neutron-rich Li and B isotopes were smaller than the standard values for the stable p - and sd -shell nuclei. Their results agreed very well with the experimental data.

Jakubassa-Amundsen [8] calculated differential cross-sections and polarization correlations for the scattering of relativistic spin polarized leptons from unpolarized ground state sodium (Na) nuclei within Distorted- Wave Born Approximation (DWBA). In addition, various nuclear ground state charge distributions were probed. Besides potential scattering, electric C2 and magnetic M1 and M3 transitions were taken into account.

In the present study, the exact center of mass correction of Mihiala-Heisenberg [9] was adopted to generate the longitudinal form factors of $^{22,26}\text{Na}$ nuclei. The longitudinal form factors, and the quadrupole moment of ^{22}Na (the ground and low-lying states) and of ^{26}Na (ground state) were re-examined to the three sd -shell interactions, USDA, USDB [10,11], and Wildenthal (W) [12] with the core-polarization effects which were included through the effective charges. The calculations included the standard and Bohr-Mottelson effective charges.

2. Theory

The longitudinal form factor for a given multipolarity L and momentum transfer \vec{q} can be written in terms of matrix elements reduced both in angular momentum and isospin spaces as [13]:

$$|F_L^{coul}(q)|^2 = \frac{4\pi}{Z^2(2J_i+1)} \left| \sum_{T=0,1} (-1)^{T_f-T_{z_f}} \begin{pmatrix} T_f & T & T_i \\ -T_{z_f} & M_T & T_{z_i} \end{pmatrix} \left\langle J_f T_f \parallel \hat{T}_L^{coul}(q) \parallel J_i T_i \right\rangle \right|^2 \tag{1}$$

$$\times |F_{c.m.}(q)|^2 \times |F_{f.s.}(q)|^2$$

Where the bracket $\begin{pmatrix} \cdot & \cdot & \cdot \\ \cdot & \cdot & \cdot \end{pmatrix}$ denotes the 3j-symbols, $F_{f.s.}(q) = [1 + (q/4.33)^2]^{-2}$ is the free

nucleon correction due to the finite size of the nucleon, and $F_{c.m.} = e^{\frac{q^2 b^2}{4A}}$ is the center of mass correction [14,15]. The many-particles reduced matrix elements of the longitudinal operator T_{LT}^{coul} between the initial (*i*) and final (*f*) states can be written as the sum of the product of the one-body density matrix (OBDM) times the single-particle matrix elements [16,13]:

$$\left\langle J_f T_f \parallel \hat{T}_{L,T}^{coul}(q) \parallel J_i T_i \right\rangle = \sum_{a,b} OBDM(L, J_f, J_i, a, b, t_z) \left\langle a \parallel \hat{T}_{L,t_z}^{coul}(q) \parallel b \right\rangle \tag{2}$$

The sum extends over all pairs of single-nucleon states (*a, b*). The OBDM (ΔT) is defined in the second quantization notation as [17]:

$$OBDM(L, a, b, f, i, \Delta T) = \frac{\left\langle f \parallel [a_{(a)}^+ \otimes \tilde{a}_{(b)}]^{(L, \Delta T)} \parallel i \right\rangle}{\sqrt{(2L+1)(2T+1)}} \tag{3}$$

The operators a^+ and \tilde{a} are the creation and annihilation operators of a neutron or proton (according to the value of t_z) in the single states *a* and *b*, respectively.

The average occupation numbers in each subshell *j* is given by [18]:

$$occ\#(j, t_z) = OBDM(a, b, t_z, L=0) \sqrt{\frac{2j+1}{2J_i+1}} \tag{4}$$

The reduced single-particle matrix elements between the final $|a\rangle$ state and the initial state $|b\rangle$ can be written as [19]:

$$\left\langle a \parallel \hat{T}_{L,t_z}^{coul} \parallel b \right\rangle = e(t_z) \left\langle n_a \ell_a \mid j_L(qr) \mid n_b \ell_b \right\rangle \left\langle \ell_a \frac{1}{2} J_a \parallel Y_L(\Omega_r) \parallel \ell_b \frac{1}{2} J_b \right\rangle \tag{5}$$

Where $j_L(qr)$ is the spherical Bessel function, $Y_L(\Omega_r)$ is the spherical harmonics function.

The electric quadrupole moment in a state $|L=2 M=0\rangle$ for $J_i = J_f$ is defined as [20]:

$$Q = \begin{pmatrix} J_i & 2 & J_i \\ -J_i & 0 & J_i \end{pmatrix} \sqrt{\frac{16\pi}{5}} \left\langle J_i \parallel \hat{O}(C2) \parallel J_i \right\rangle \tag{6}$$

Where, $\left\langle J_i \parallel \hat{O}(C2) \parallel J_i \right\rangle$ is the nuclear matrix element of the electromagnetic operators.

The Translation Invariant Shell Model (TISM) provides a proper description for electron scattering process. The wave function is factorized into center of mass wave function being a Gaussian and an intrinsic wave function of relative coordinates. This allows calculating the form factor in the form [21]

$$F(q) = e^{-b^2 q^2 / 4A} F_{int}(q) \tag{7}$$

The calculation usually gives the form factor of one-body density labeled $F(q)$, whereas the experiment requires the form factors with respect to the center of mass, labeled $F_{int}(q)$. The form factor at momentum transfer q in Born approximation is given by [14, 9]

$$F_{int}(\vec{q}) = \left\langle \phi_0 \left| \sum_k f_k(q^2) e^{i\vec{q} \cdot \vec{r}'_k} \right| \phi_0 \right\rangle \tag{8}$$

Where ϕ_0 is the translation invariant ground state, \vec{r}'_k is the distance from the center of mass to the k^{th} "point" nucleon, ($\vec{r}'_k = \vec{r}_k - \vec{R}_{c.m}$), $k = 1, 2, \dots, A-1$, and $f_k(q^2)$ is the nucleon form factor which takes into account the finite size of the nucleon k .

The form factor can be calculated by carrying out an expansion in terms of many-body operators [21]

$$F_{int}(\vec{q}) = \sum_k f_k(q^2) \left\langle e^{i\vec{q} \cdot \vec{r}_k (A-1)/A} \prod_{m \neq k} [1 + f^*(\vec{q} \cdot \vec{r}_m / A)] \right\rangle \tag{9}$$

The many-body expansion for the form factor F_{int} takes the following form,

$$\begin{aligned} F_{int}(\vec{q}) &= \sum_k f_k(q^2) \left\langle e^{i\vec{q} \cdot \vec{r}_k (A-1)/A} \right\rangle \\ &+ \sum_k f_k(q^2) \sum_{m \neq k} \left\langle e^{i\vec{q} \cdot \vec{r}_k (A-1)/A} f^*(\vec{q} \cdot \vec{r}_m / A) \right\rangle \\ &+ \frac{1}{2} \sum_k f_k(q^2) \sum_{m, n \neq k} \left\langle e^{i\vec{q} \cdot \vec{r}_k (A-1)/A} f^*(\vec{q} \cdot \vec{r}_m / A) \right\rangle \times f^*(\vec{q} \cdot \vec{r}_n / A) + \dots \end{aligned} \tag{10}$$

With the exact value of the center of mass correction introduced in TISM, the form factor given in Eq. (1) becomes:

$$\begin{aligned} |F_J^m(q)|^2 &= \frac{4\pi}{Z^2(2J_i + 1)} \left| \sum_{T=0,1} (-1)^{T_f - T_{fz}} \begin{pmatrix} T_f & T & T_i \\ -T_{zf} & M_T & T_{zi} \end{pmatrix} \left\langle J_f T_f \parallel \hat{T}_L^m(q) \parallel J_i T_i \right\rangle \right|^2 \\ &\times |F_{int}(q)|^2 \times |F_{f..s}(q)|^2 \end{aligned} \tag{11}$$

In the present work, $F_{int}(q)$ was calculated from Eq. (10) and denoted by green curve in Figure 4. More details were performed by Mihaila and Heisenberg [9]. The present calculations are carried out by use of the OXBASH shell model code [22].

3. Results and Discussion

The longitudinal form factors for the elastic electron scattering from $^{22,26}\text{N}$ nuclei were performed. Three *sd*-shell interactions; USDA, USDB and Wildenthal were used to calculate the longitudinal transitions matrix elements and quadrupole moments(Q) of the ground and excited states of $^{22,26}\text{Na}$ nuclei. The calculated values of Q were compared with the available measured values [23] as well as with the other results and are listed in Table 1. The measured Q are systematically larger than those calculated with bare nucleon charges. This is due to the well-known effect of the polarization of the core protons by the valence protons and neutrons [24,25]. This effect can be calculated by replacing the free nucleon charges with effective charges $e_p^{eff} = 1 + \delta e_p$ & $e_n^{eff} = 0 + \delta e_n$, where δe are the polarization charges. All theoretical studies result in $\delta e_n > \delta e_p$ [24,25], because the valence neutrons are more effective in polarization of the core protons due to the stronger average p-n interaction compared to the p-

p interaction. The sensitivity of Q to the values of effective charges are presented with $e_p=1.35$, $e_n=0.35$ [26], and with Bohr Mottelson formula, which is given by [27]:

$$e^{eff}(t_z) = e(t_z) + e \delta e(t_z) \quad (12)$$

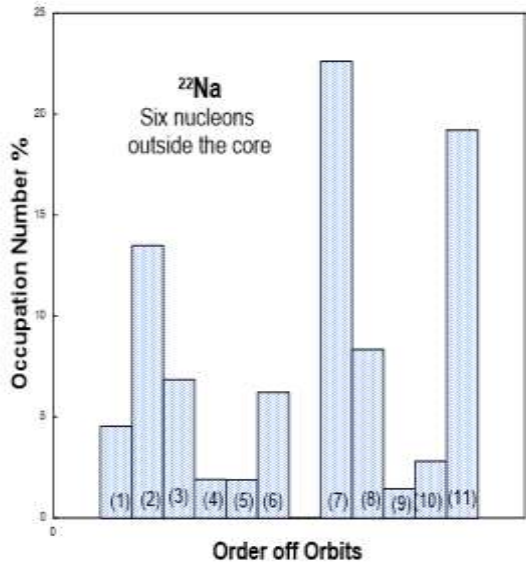
$$\delta e(t_z) = Z/A - 0.32(N-Z)/A - 2t_z[0.32 - 0.3(N-Z)/A] \quad (13)$$

The calculations incorporated the single – particle wave functions of harmonic oscillator potential with size parameter b. The size parameter b for the nuclei under consideration was calculated as: $b = \sqrt{\frac{\hbar}{M_p \omega}}$; $\hbar \omega = 45 A^{-1/3} - 25 A^{-2/3}$, where M_p is the mass of proton [16]. The exact value of the center of mass corrections in TISM was also examined.

3.1 The ^{22}Na Nucleus ($\mathbf{J}^\pi\mathbf{T} = \mathbf{3}^+\mathbf{0}$, $\tau_{1/2} = 2.6$ y)

The ground state of ^{22}Na nucleus is specified by $\mathbf{J}^\pi\mathbf{T} = \mathbf{3}^+\mathbf{0}$ with half-life of $\tau_{1/2} = 2.6$ y [23], has the configurations of $(1s)^4$, $(1p_{3/2})^8$, $(1p_{1/2})^4$ inert core (^{16}O), with USDA interaction [11]. A clear configuration mixture in this state is shown in Figure 1, where the occupation numbers percentages are calculated and presented. The elastic longitudinal form factors with the size parameter $b = 1.795\text{fm}$ were calculated for USDA, USDB and W *sd*-shell interactions. Figure 2 shows the *sd*-shell model space form factors for USDA interaction with bare charge (black solid curve). The contributions of C0 (short-dashed curve), C2 (long-dashed curve) and C4 (dashed-dot curve) components are also indicated. The C0 component exhibits two diffraction minimum located at $q=1.5\text{fm}^{-1}$ and $q=2.8\text{fm}^{-1}$, and the C2 component is dominant at low q -region with diffraction minimum located at $q=1.7\text{fm}^{-1}$, while the C4 component is peaked around at $\sim 10^{-5}$ value, and has minor effect compared with the other components. No experimental data is available for this transition. The total longitudinal form factors with bare charge for the three *sd*-interactions USDA (black curve), USDB (red curve) and W (blue curve) are identical having the same behavior as shown in Figure 3, and are dominant at low q region, with diffraction minimum located at $q \sim 1.5 \text{ fm}^{-1}$. The comparison of the elastic longitudinal form factors with and without the exact center of mass correction for each interaction separately are shown in Figure 4 (green and black curves respectively), and labeled by (a) for USDA, (b) for USDB and (c) for W. There is a significant enhancement in the form factors with the exact center of mass correction (green curve) especially for $q > 2.0 \text{ fm}^{-1}$. The inclusion of the core polarization effects with different effective charges for USDA interaction without center of mass correction are shown in Figure 5. The longitudinal form factors with bare charge (black curve) are compared with that of effective charge $e_p=1.35e$ and $e_n=0.35e$ (dashed curve), and with that of $e_p=1.18e$ and $e_n=0.82e$ (dashed dot curve). The inclusion of core polarization effects slightly increased the form factors at $q > 2.0 \text{ fm}^{-1}$. The core polarization effects are included through the calculated effective charge $e_p=1.18e$ and $e_n=0.82e$. This inclusion with the exact center of mass correction is displayed in Figure 6 for different interactions; USDA (black curve), USDB (red curve) and W (blue curve). Minor effect for the core polarization contribution on the magnitude of the total form factors for all interactions and for all q -values in comparison with the model space results are shown in Figure 3. The calculation of the quadrupole moment was based on the full *sd*-model space wave functions ($1d_{5/2}$, $2s_{1/2}$, $1d_{3/2}$) with USDA, USDB and W interactions. The measured quadrupole moment $Q_{exp.} = 18.5(11) \text{efm}^2$ [23] was reproduced in sign, but overestimated in magnitude with bare charges results for all dependent interactions. The predicted values $Q_{USDA}=12.49\text{efm}^2$, $Q_{USDB}=12.55\text{efm}^2$, and $Q_W=12.62\text{efm}^2$ are presented in Table 1 in comparison with the experimental data and other results. The inclusion of the core polarization effect enhanced the values of quadrupole moments to be with the effective

charges $e_p=1.35e$ and $e_n=0.35e$, $Q_{USDA}=21.23\text{efm}^2$, $Q_{USDB}=21.34\text{efm}^2$, $Q_W=21.45\text{efm}^2$, and for $e_p=1.18e$ and $e_n=0.82e$, $Q_{USDA}=24.97\text{efm}^2$, $Q_{USDB}=25.11\text{efm}^2$, and $Q_W =25.24\text{efm}^2$. These results are close to each other and give a reasonable agreement with the measured value within the experimental error.



- 1) $1d_{3/2}= 2, 1d_{5/2}= 3, 2s_{1/2}= 1$; 2) $1d_{3/2}= 1, 1d_{5/2}= 4, 2s_{1/2}= 1$
- 3) $1d_{3/2}= 2, 1d_{5/2}= 4, 2s_{1/2}= 0$; 4) $1d_{3/2}= 3, 1d_{5/2}= 3, 2s_{1/2}= 0$
- 5) $1d_{3/2}= 2, 1d_{5/2}= 2, 2s_{1/2}= 2$; 6) $1d_{3/2}= 1, 1d_{5/2}= 3, 2s_{1/2}= 2$
- 7) $1d_{3/2}= 0, 1d_{5/2}= 5, 2s_{1/2}= 1$; 8) $1d_{3/2}= 0, 1d_{5/2}= 4, 2s_{1/2}= 2$
- 9) $1d_{3/2}= 1, 1d_{5/2}= 2, 2s_{1/2}= 3$; 10) $1d_{3/2}= 0, 1d_{5/2}= 3, 2s_{1/2}= 3$
- 11) $1d_{3/2}= 0, 1d_{5/2}= 6, 2s_{1/2}= 0$

Figure 1: The occupation numbers percentage for the ground states of $1d_{3/2}$, $1d_{5/2}$, $2s_{1/2}$ orbits outside the ^{16}O core of considered ^{22}Na nucleus.

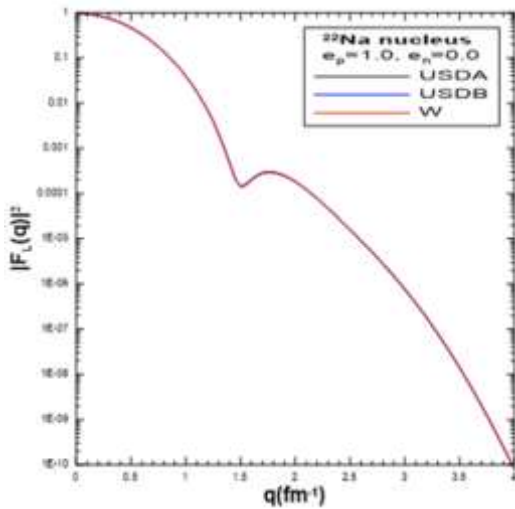


Figure 2: The elastic longitudinal form factors for ^{22}Na ground state calculated in sd-model space only. The individual multipole contributions of C0, C2, and C4 are shown.

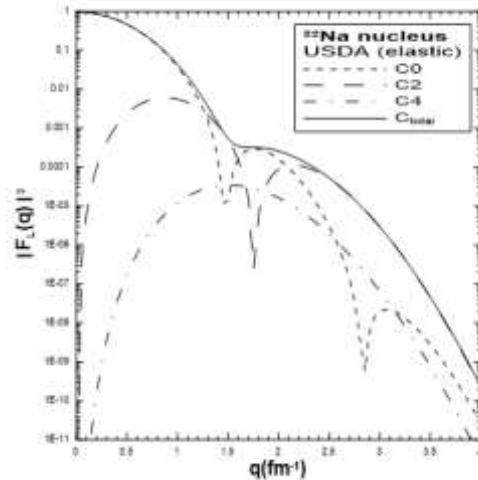


Figure 3: Elastic longitudinal form factors of ^{22}Na nucleus with bare charge for USDA (black curve), USDB (blue curve), and W- interaction (red curve).

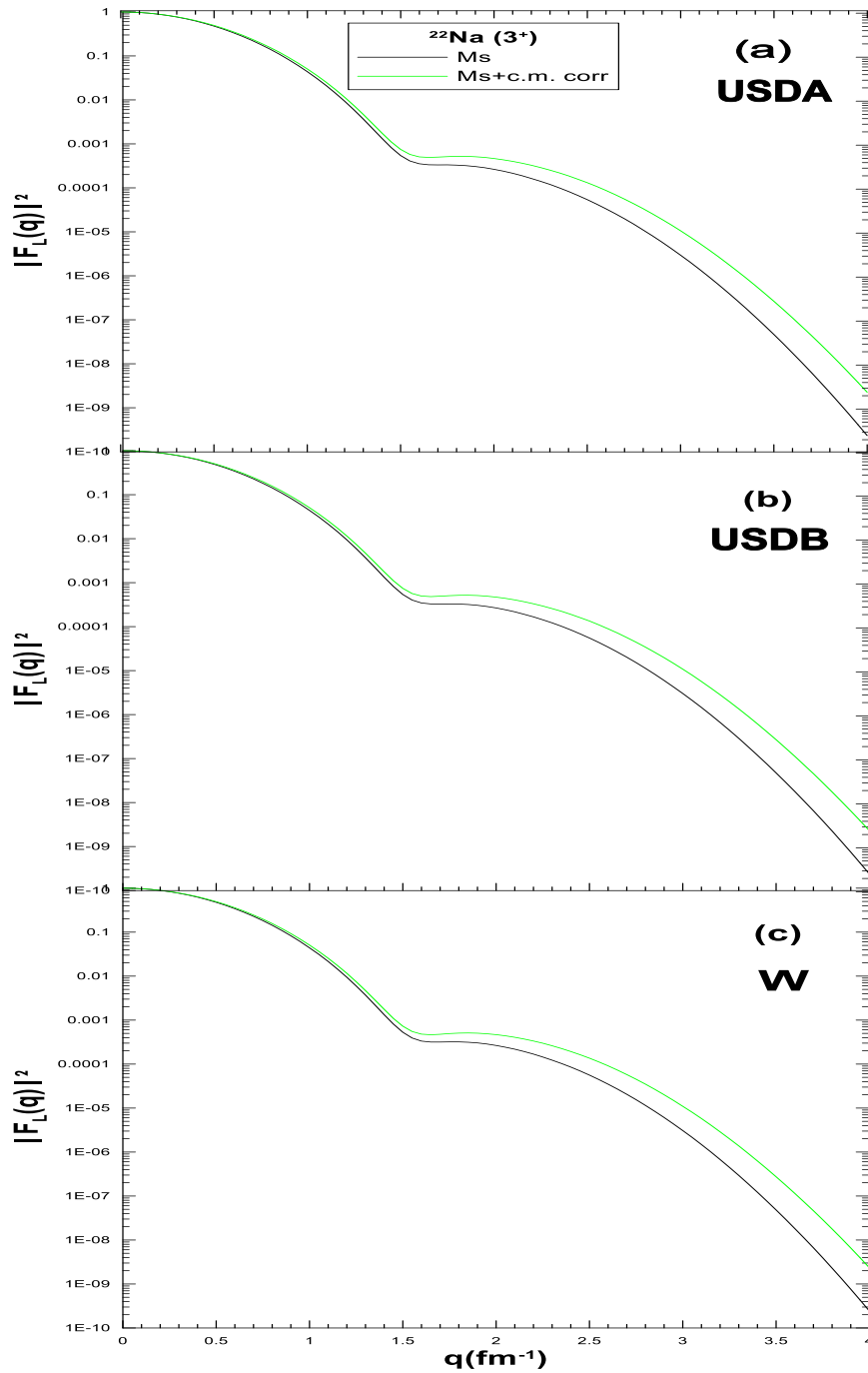


Figure 4: Comparison between the total form factors of ^{22}Na ground state without c.m. corr. (black curve) and with c.m corr. (green curve) for USDA (a), USDB (b), and W (c) separately.

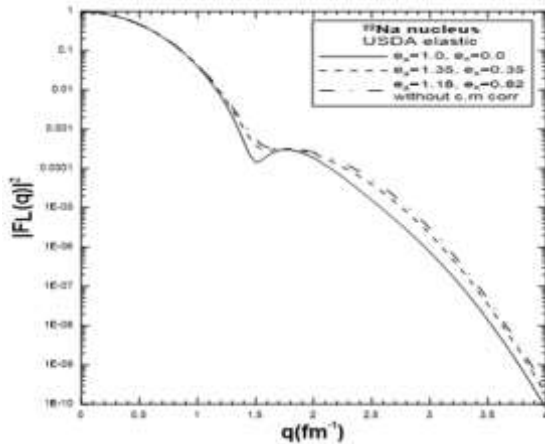


Figure 5: comparison between the total form factors of ^{22}Na ground state without c.m.corr. for different effective charges for USDA interaction.

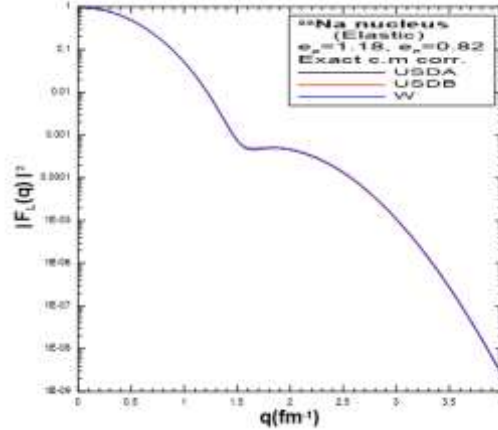


Figure 6: Comparison between the total form factors of ^{22}Na ground state in model space with effective charge with center of mass correction for three interactions USDA (black curve), USDB (red curve), and W (blue curve).

3.2 ^{22}Na Nucleus ($J^\pi T = 1^+ 0$, $\tau_{1/2} = 243\text{ns}$, $E_x = 583\text{keV}$)

The inelastic electron scattering from ^{22}Na excited state ($J^\pi T = 1^+ 0$, $E_x = 583\text{keV}$) is purely isoscalar. The longitudinal form factors for sd -shell model space with $b = 1.795\text{fm}$ were calculated using the universal sd -shell interaction (USDA) [11] and are shown in Figure 7 (solid curve). The C2 form factor (dashed curve) is dominant at the low (q) region with diffraction minimum located at $q \sim 2.3\text{fm}^{-1}$, and the C4 component (dashed dot curve) is marginally moved forward with diffraction maximum position around $q \sim 1.6\text{fm}^{-1}$ with a height of the order $\sim 10^{-7}$. The comparison of the calculated longitudinal form factors with bare charges and without the exact center of mass correction for three different interactions is displayed in Figure 8, for USDA (black curve), USDB (red curve) and W-interaction (blue curve). The calculations of USDA interaction are similar to that of W-interaction at low range of momentum transfer ($q < 1.5\text{fm}^{-1}$), and similar to that of USDB interaction at high q -region ($q > 3.0\text{fm}^{-1}$). The calculations of USDB-interaction have a diffraction maximum of height lower than that of the others calculations. The dependence of the longitudinal form factors with the exact center of mass correction (green curve) and without the exact center of mass correction (black curve) for (a) USDA, (b) USDB and (c) W-interactions are indicated separately in Figure 9. It is obvious that the exact center of mass correction (green curve) has increased the form factor for each interaction along with the range of $q > 1.5\text{fm}^{-1}$. USDA and USDB-interactions gave similar descriptions along all ranges of q , but the result of W interaction (green curve) distinctly differed from that of USDA and USDB in the region of ($1.5 < q < 2.3\text{fm}^{-1}$). The core polarization effects with the different effective charges for USDA interaction and without center of mass correction are shown in Figure 10. The results obtained with $e_p = 1.35e$ and $e_n = 0.35e$ (dashed curve), and with $e_p = 1.18e$ and $e_n = 0.82e$ (dashed dot curve) have significant enhancement on the form factors along all range of q compared with that of bare charges (black curve), and play a distinct role on the values of quadrupole moment. The contributions of the effective charges $e_p = 1.18e$ and $e_n = 0.82e$ with the exact center of mass correction are depicted in Figure 11 for USDA (black curve), USDB (red curve) and W-interaction (blue curve). These interactions gave essentially the same behavior for the form factors, in comparison to that of bare charges shown in Figure 8, the curves slightly shifted upward with different heights of diffraction maximum for each interaction. The diffraction maximum of USDA and W-interactions are located at $q \sim 1\text{fm}^{-1}$ and have the

same height of the order $> 10^{-6}$, while the diffraction maximum of USDB-interaction is located at $q \sim 1.3 \text{ fm}^{-1}$ with height of the order $> 10^{-7}$. The calculated quadrupole moments for three sd-shell interactions with bare charges, $Q_{\text{USDA}} = 6.139 \text{ efm}^2$, $Q_{\text{USDB}} = 6.144 \text{ efm}^2$, and $Q_{\text{W}} = 6.071 \text{ efm}^2$ are close to each other. The inclusion of the core excitation with effective charge $e_p = 1.35e$ and $e_n = 0.35e$ enhances the values by about a factor of 1.5, to be, $Q_{\text{USDA}} = 10.44 \text{ efm}^2$, $Q_{\text{USDB}} = 10.44 \text{ efm}^2$, and $Q_{\text{W}} = 10.32 \text{ efm}^2$. The results are enhanced by about a factor of 2 with effective charge $e_p = 1.18e$ and $e_n = 0.82e$, to be $Q_{\text{USDA}} = 12.28 \text{ efm}^2$, $Q_{\text{USDB}} = 12.29 \text{ efm}^2$, and $Q_{\text{W}} = 12.14 \text{ efm}^2$. No measured value for this is available to be compared with. These values of Q moments are tabulated in Table 1.

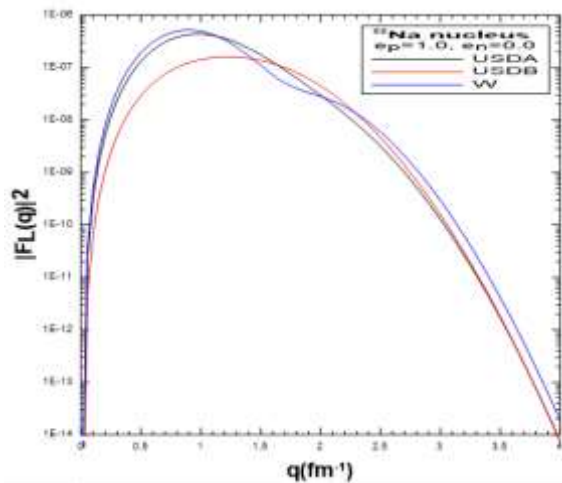


Figure 7: The longitudinal form factors for ^{22}Na excited state calculated in psd-model space only (MS). The component C2 and C4 are shown

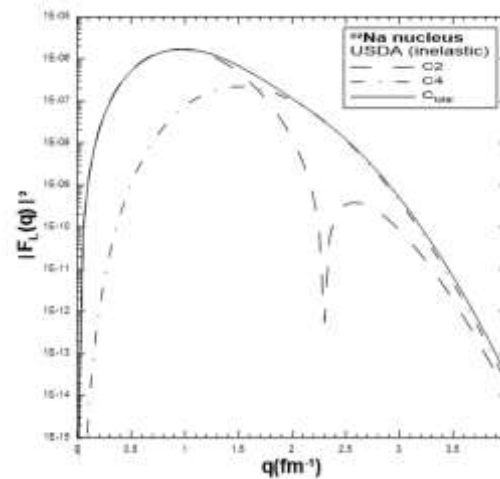


Figure 8: Comparison between the total form factors of ^{22}Na excited state in model space only with bare charge between USDA (black curve), USDB (red curve), and W (blue curve) interactions.

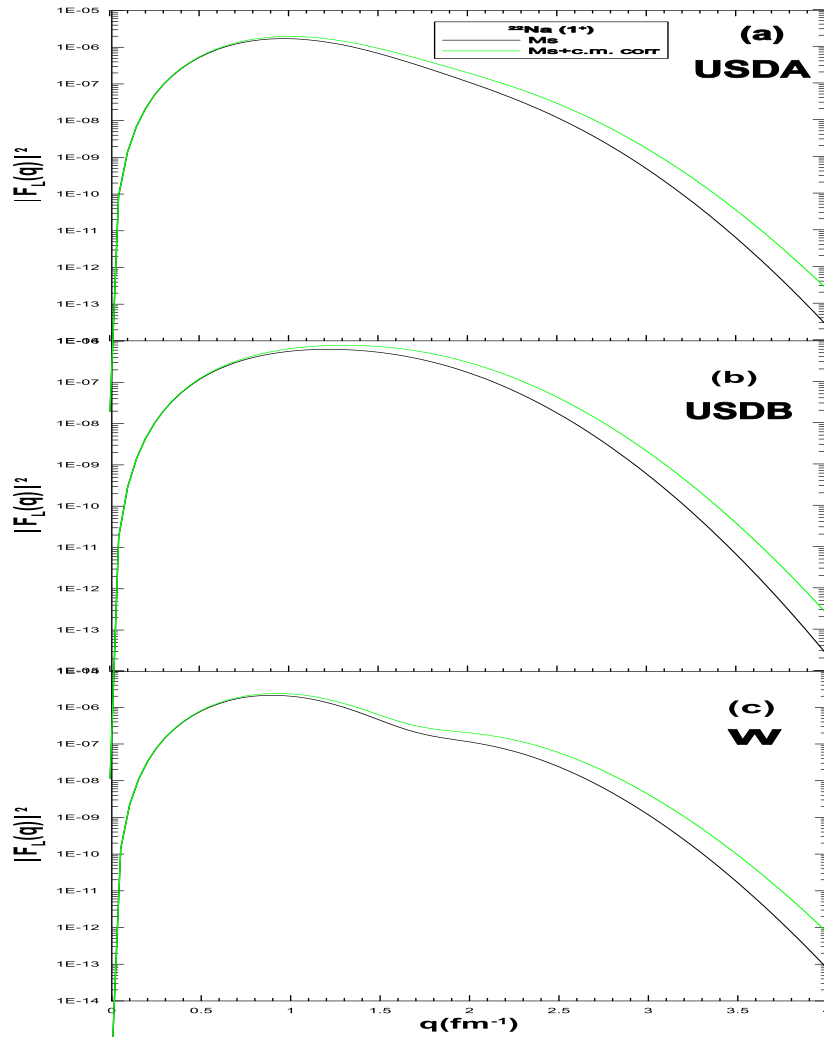


Figure 9: Comparison between the total form factors of ^{22}Na excited state without c.m. corr. (black curve) and with c.m. corr. (green curve) for USDA (a), USDB (b), and W (c) separately.

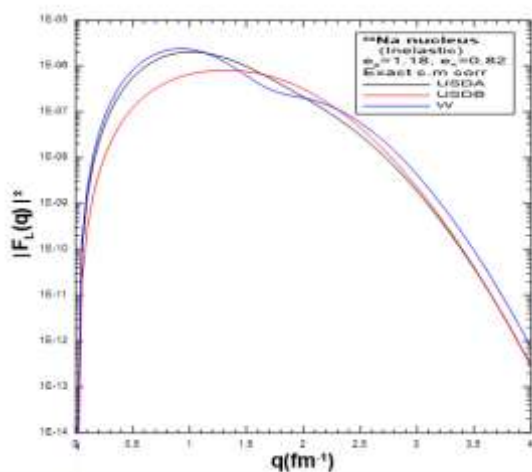


Figure 10: Core polarization effect on the total form factors of ^{22}Na excited state with different effective charges for USDA interaction.

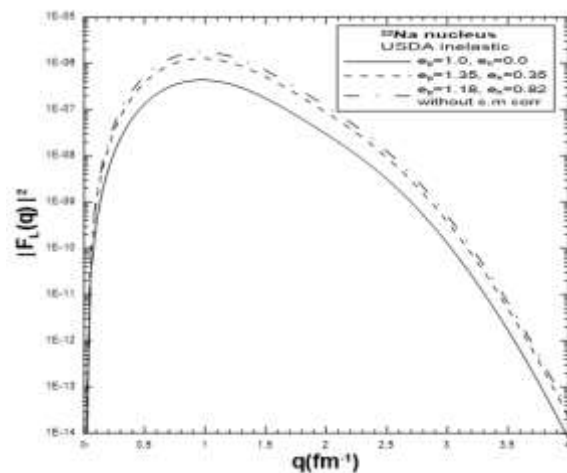


Figure 11: Comparison between the total form factors of ^{22}Na excited state for model space with center of mass correction (MS + CP) for interactions USDA (black curve), USDB (red curve), and W (blue curve).

3.3 ^{26}Na Nucleus ($J^{\pi}T = 3^{+}2$, $\tau_{1/2} = 1.07$ s)

The ground state of ^{26}Na nucleus (neutron rich) is characterized by $J^{\pi}T = 3^{+}2$, with half-life $\tau_{1/2} = 1.07$ s [23]. The configurations used to describe the ground state of ^{26}Na nucleus with USDA interaction [11] are $(1s)^4$, $(1p_{3/2})^8$, $(1p_{1/2})^4$ inert core, with ten nucleons distributed over $1d_{5/2}$, $2s_{1/2}$ and $1d_{3/2}$ orbits. The results of a clear configuration mixture with occupation numbers percentages are shown in Figure 12. The configuration of the dominant component has the form $(1d_{3/2})^0 (1d_{5/2})^9 (2s_{1/2})^1$. The calculated longitudinal form factors of the sd -shell model space (MS) with $b = 1.834\text{fm}$ are presented in Figure 13 (black solid curve) for USDA interaction. The individual components C0 (short dashed curve) C2 (long dashed curve) and C4 (dashed-dot curve) are shown. No experimental data are available for the longitudinal form factors of this state. The quadrupole and hexadecupole dominated at around $q \sim 1.0\text{fm}^{-1}$ and $q \sim 1.6\text{fm}^{-1}$ regions, respectively with the same height of the order $> 10^{-6}$. While the dominant contribution of C0 component appears at low q -region with two diffraction minima located at $q \sim 1.3\text{fm}^{-1}$ and 3.0fm^{-1} respectively. In the region of $(0.1 < q < 3.0)\text{fm}^{-1}$, the total longitudinal form factors are almost due to C0 transition. The inclusion of the exact center of mass correction (green curve) enhanced the total form factors at $q > 1.5\text{fm}^{-1}$ region. The total longitudinal form factors with bare charge and without the exact center of mass correction are depicted in Figure 14 for three sd -shell interactions, USDA (black curve), USDB (blue curve) and W (red curve). All three interactions have the same behavior and dominate at the same regions of q , with minor enhancement from W- interaction for the form factors along the region of q ($2.8 < q < 3.7$) fm^{-1} . The calculated longitudinal form factors (with $e_p=1$, $e_n=0$) with and without the exact center of mass correction were separately compared for three sd -shell interactions as shown in Figure 15 (green and black curves respectively), and denoted by (a) for USDA, (b) for USDB and (c) for W-interaction. It is clear that the inclusion of the exact center of mass correction gives the same enhancement to the form factors for all three interactions at the range of momentum transfer $q > 1.5\text{fm}^{-1}$. The core polarization effects were included with different effective charges for USDA interaction and without the exact center of mass correction. This comparison is shown in Figure 16. The results obtained for purely isoscalar effective charges with $e_p=1.35e$ and $e_n=0.35e$ (blue curve), and with $e_p=1.1e$ and $e_n=0.647e$ (red curve) have no significant effect on the magnitude of the longitudinal form factors along all range of q compared with that of bare charges (black curve). The remaining systematic enhancement of the longitudinal form factors with the exact center of mass correction are shown in Figure 17. The core excitations play distinct role on the values of quadrupole moment. The calculated quadrupole moments (Q) with free charges $Q_{\text{USDA}} = -0.489\text{efm}^2$, $Q_{\text{USDB}} = -0.446\text{efm}^2$ and $Q_{\text{W}} = -0.797\text{efm}^2$, are close to the measured value $Q_{\text{exp.}} = -0.53(2)\text{efm}^2$ [23], especially for USDA interaction, and with some enhancement for W interaction. The measured value is nicely confirmed for USDA interaction with $e_p=1.35e$ and $e_n=0.35e$, $Q_{\text{USDA}} = -0.522\text{efm}^2$, and well reproduced within the experimental error for USDB and W interactions, $Q_{\text{USDB}} = -0.488\text{efm}^2$ and $Q_{\text{W}} = -1.138\text{efm}^2$, as tabulated in Table 1. The calculated quadrupole moments with Bohr Mottelson (BM) effective charges, $e_p=1.1e$ and $e_n=0.647e$, $Q_{\text{USDA}} = -0.283\text{efm}^2$, $Q_{\text{USDB}} = -0.280\text{efm}^2$ and $Q_{\text{W}} = -0.991\text{efm}^2$, are reduced by a factor of approximately one half compared with the measured value. The small Q of ^{26}Na is due to the fact that the configuration of the dominant component of the wave functions has the form $(1d_{5/2})^3$ for protons and $(1d_{5/2})^6, (2s_{1/2})^{0-2}$ for neutrons. For this main configuration, the neutrons and the protons have zero Q , because the valence neutrons outside the $1d_{5/2}$ closed shell are in the $2s$ state, and the protons are in the middle of a j -shell [17].

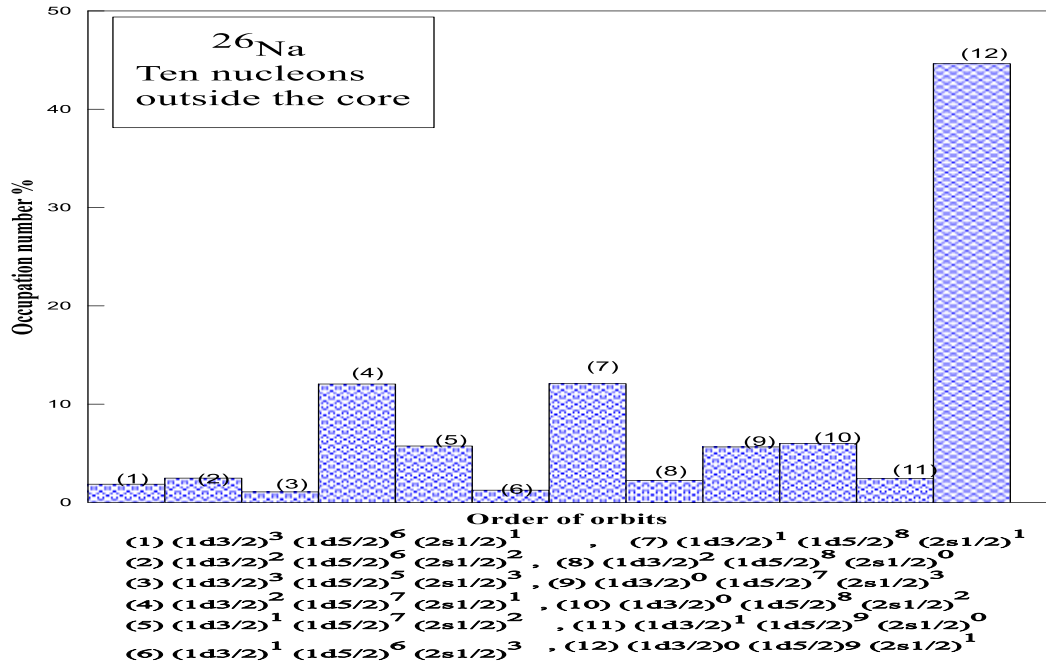


Figure 12: The occupation numbers percentage for the ground states of $1d_{3/2}$, $1d_{5/2}$, $2s_{1/2}$ orbits outside the ^{16}O core of considered ^{26}Na nucleus.

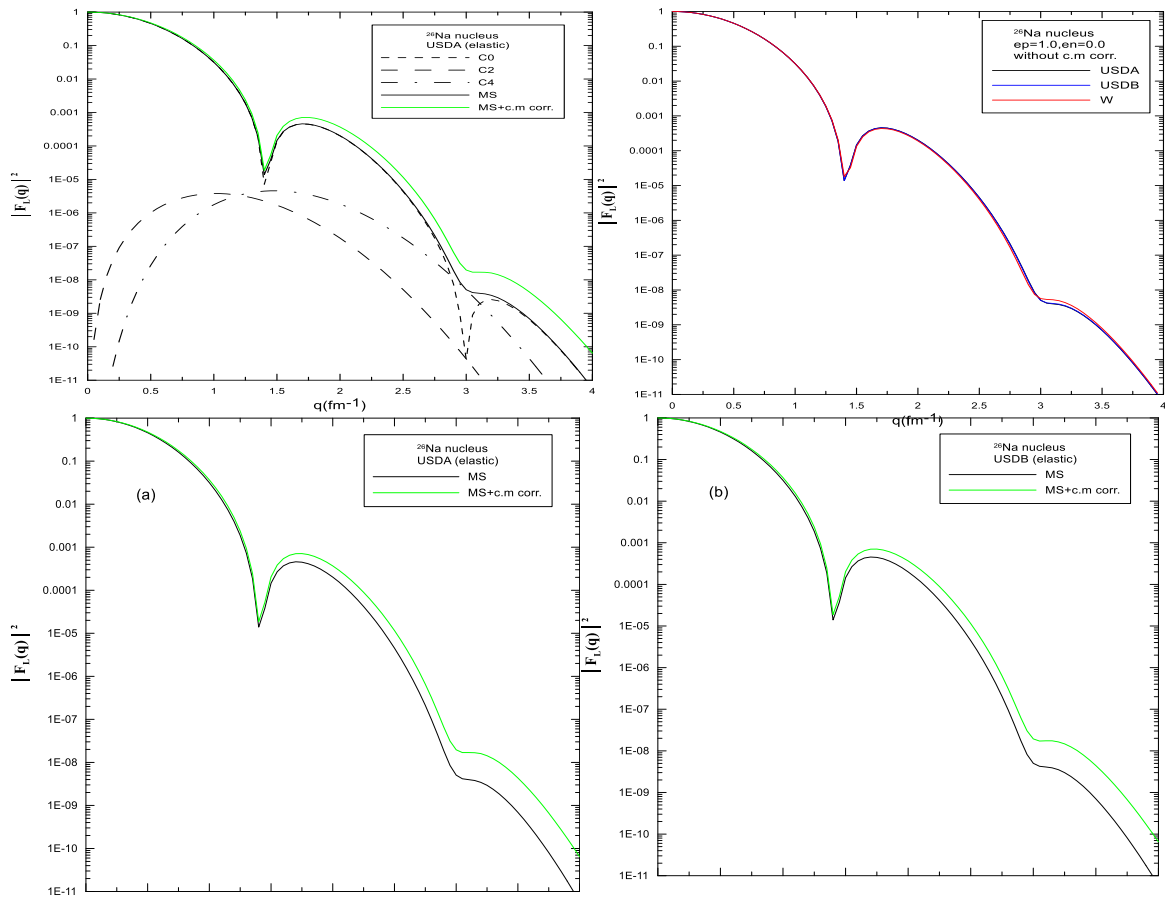


Figure 13: The longitudinal form factors for ^{26}Na ground state calculated in sd -model space (black solid curve) and with $e_{(free)}+c.m.$ corr. (green curve). The individual multipole contribution of C0, C2 and C4 are shown.

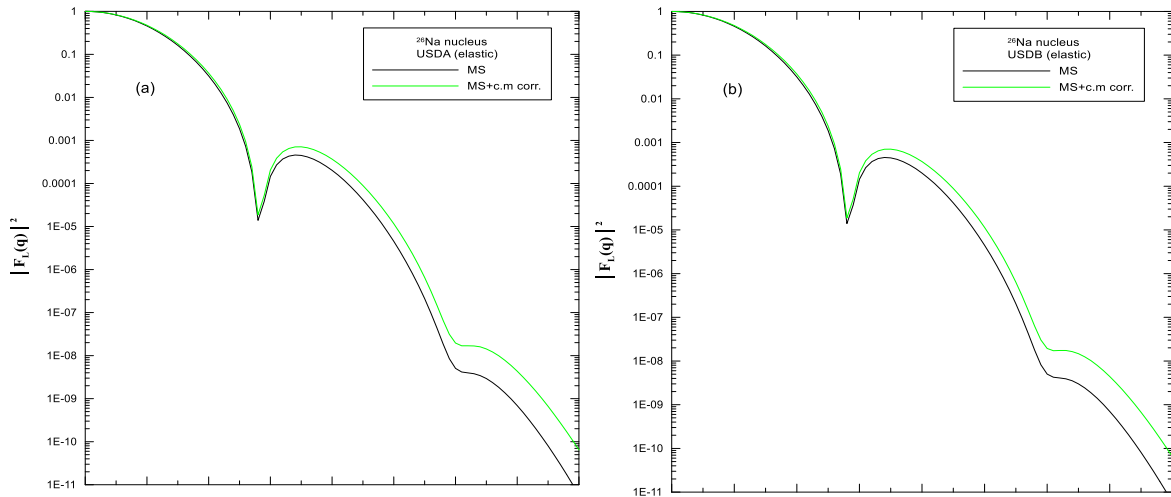


Figure 14: Elastic longitudinal form factors of ^{26}Na nucleus with $e_{(\text{free})}$ for USDA (black curve), USDB (blue curve), and W-interaction (red curve).

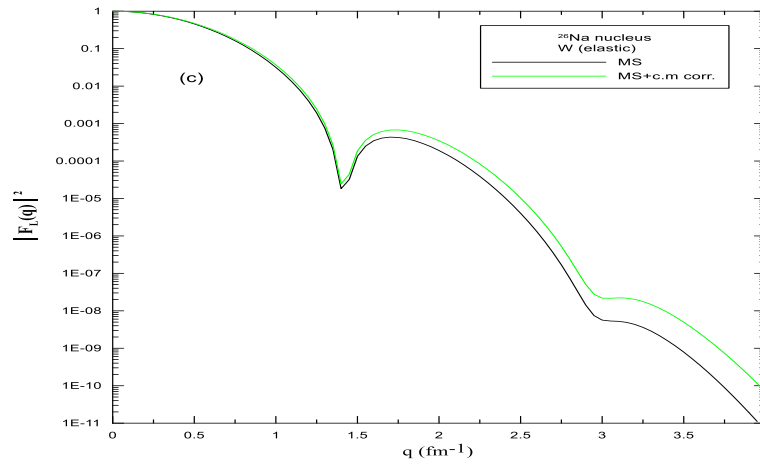


Figure 15: Comparison between the total form factors of ^{26}Na nucleus without c.m. corr. (black solid curve) and with c.m. corr. (green curve) for (a) USDA, (b) USDB, and (c) W interactions.

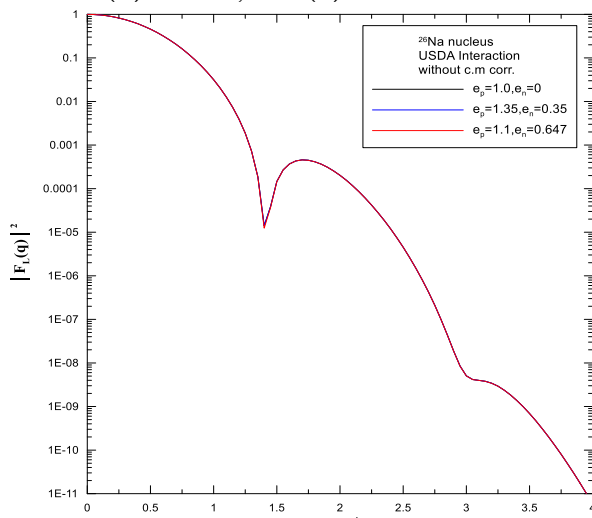


Figure 16: Comparison between the total form factors using the USDA -interaction of ^{26}Na nucleus with difference $e_{(\text{eff.})}$ without c.m corr.

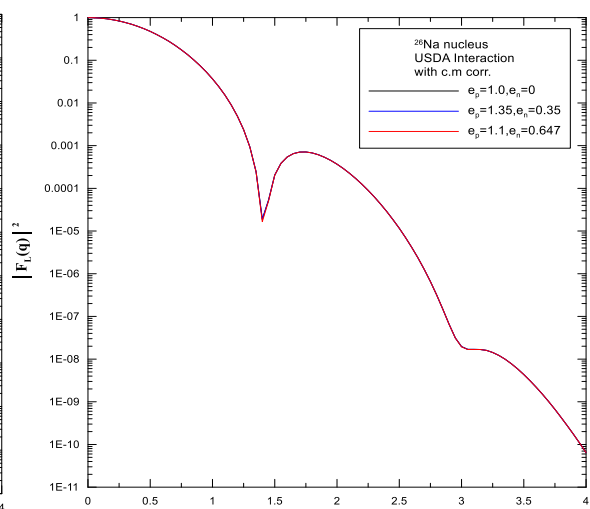


Figure 17: Comparison between the total form factors using the USDA -interaction of ^{26}Na nucleus with difference $e_{(\text{eff.})}$ with c.m corr.

Table 3.2: The calculated quadrupole moments of ^{22}Na and ^{26}Na nuclei are compared with experimental results and with other results

Nucleus	J^π	E_x (keV)	b (fm)	Effective Charges	$Q_{\text{Calc.}}(efm^2)$ using USDA interaction	$Q_{\text{Calc.}}(efm^2)$ using USDB interaction	$Q_{\text{Calc.}}(efm^2)$ using W interaction	$Q_{\text{exp.}}(efm^2)$	Other Result (efm^2)
^{22}Na	3^+	0	1.795	$e_p=1.0, e_n=0.0$	12.49	12.55	12.62	18.0(11) [23] 18.5±1.1 [28]	23.2 [29]
				$e_p=1.35, e_n=0.35$	21.23	21.34	21.45		
				$e_p=1.18, e_n=0.82$	24.97	25.11	25.24		
^{22}Na	1^+	583	1.795	$e_p=1.0, e_n=0.0$	6.139	6.144	6.071		
				$e_p=1.35, e_n=0.35$	10.44	10.44	10.32		
				$e_p=1.18, e_n=0.82$	12.28	12.29	12.14		
^{26}Na	3^+	0	1.834	$e_p=1.0, e_n=0.0$	-0.489	-0.446	-0.797	- 0.53(2)[23] 3]	-0.4 [29]
				$e_p=1.35, e_n=0.35$	-0.522	-0.488	-1.138		
				$e_p=1.1, e_n=0.64$	-0.283	-0.280	-0.991		

3. 4 Conclusions

Analysis calculations for the $^{22,26}\text{Na}$ nuclei showed a strong contribution of $1d_{5/2}$ orbit, for all C2 transitions. The inclusion of the exact value of center of mass correction has a reasonable contribution on q dependence form factors and a minor role on the quadrupole values, whereas, the inclusion of effective charges was adequate to obtain a good agreement between the predicted and measured quadrupole moment. Also, all three sd -shell interactions gave a similar description to the longitudinal form factors of Na-isotopes, since $^{22,26}\text{Na}$ are exotic nuclei near the stability, and the small Q moment of ^{26}Na is due to the dominant configuration in which the neutrons and proton have zero Q, since the valence neutrons outside the closed shell are in the $2s$ state, and the protons are in the middle of a j -shell.

References

- [1] N. C. Summers, G. Hackman, T. E. Drake, C. Andreoiu, R. Asley, G. C. Ball, P. C. Bender, A. J. Boston, H. C. Boston, A. Chester, A. Close, D. Cline, D. S. Cross, R. Dunlop, A. Finley, A. Garnsworthy, A. B. Hayes, A. Laffoley, T. Nano, P. Voss, S. J. Williams, Z. M. Wang "B(E1) strengths from Coulomb excitation of ^{11}Be " *Phys. Lett. B*, 650, 124-128, 2007.
- [2] H. Uberall; "Electron Scattering Form Complex Nuclei" *Academic press*, New York, 1971.
- [3] M. Keim, U. Georg, A. Klein, R. Neugart, M. Neuroth, S. Wilbert, P. Lievens, L. Vermeeren, B. A. Brown & ISOLDE Collaboration "Measurement of the electric quadrupole moments of $^{26-29}\text{Na}$ " *Eur. Phys. J. A*, vol. 8, 31-40, 2000.
- [4] Z. A. Dakhil, B. S. Hameed "The Electro-Excitation Form Factors of ^7Li Nucleus with Exact Center of Mass Correction" *Iraqi J of Physc.*, vol. 8, no. 13, PP. 38-44, 2010.
- [5] X. Roca-Maza, M. Centelles, F. Salvat, and X. Vinas "Theoretical study of elastic electron scattering off stable and exotic nuclei" *Phys. Rev. C*, vol. 78, 044332, 2008.
- [6] X. Roca-Maza, M. Centelles, F. Salvat, and X. Vinas "Electron scattering in isotonic chains as a probe of the proton shell structure of unstable nuclei" *Phys. Rev. C*, vol.87, 014304, 2013.

- [7] R. A. Radhi, Z. A. Dakhil and N. S. Manie "Quadrupole Moment of ^{14}B Exotic Nucleus" *Iraqi J of Physc.* vol.12, No.23, 44-50, 2014.
- [8] D. H. Jakubassa-Amundsen "Elastic scattering of spin-polarized electrons and positrons from ^{23}Na nuclei" *Nucl. Phys., A*, vol. 975, 107–121, 2018.
- [9] Bogdan Mihaila and Jochen H. Heisenberg "Center-of-mass corrections reexamined: A many-body expansion approach" *Phys. Rev., C*, vol. 60, 054303, 1999. Item., "Ground state correlations and mean field in ^{16}O II. Effects of a three-nucleon interaction" *Phys. Rev., C*, vol. 61, 054309, 2000. Item., "Microscopic Calculation of the Inclusive Electron Scattering Structure Function in ^{16}O " *Phys. Rev., Lett.*, vol. 84, no.7, 1403, 2000.
- [10] B. A. Brown, B. H. Wildenthal "Status of the Nuclear Shell Model" *Annu. Rev. Nucl. Part. Sci.*, vol. 38, 29-66, 1988.
- [11] B. A. Brown and W. A. Richter "New "USD" Hamiltonians for the sd shell" *Phys. Rev. C*, vol. 74, 034315, 2006.
- [12] B. H. Wildenthal "Nuclear magnetic properties and gamow-teller transitions" *Prog. Part. Nucl. Phys.*, vol. 11, 53-89, 1984.
- [13] R. A. Radhi, A. A. Abdulla, Z. A. Dakhil and N. M. Adeeb "Core-polarization effects on C2 form factors of p-shell nuclei" *Nucl. Phys., A*, 696, 442-452, 2001.
- [14] L. J. Tassie and F. C. Barker "Application to Electron Scattering of Center-of-Mass Effects in the Nuclear Shell Model" *Phys. Rev.*, 111, 940, 1958.
- [15] P. Glickman, W. Bertozzi, T. N. Buti, S. Dixit, F. W. Hersman, C. E. Hyde-Wright, M. V. Hynes, R. W. Lourie, B. E. Norum, J. J. Kelly, B. L. Berman, and D. J. Millener "Electron Scattering from ^9Be " *Phys. Rev. C* 43, 1740, 1991.
- [16] P.J. Brussard and P. W. M. Glademans, "Shell-model Application in Nuclear Spectroscopy", North-Holland Publishing Company, Amsterdam, 1977.
- [17] A. De-shalit and H. Feshbach, "*Theoretical Nuclear Physics*", vol.1: Nuclear Structure", John and Sons, New York, 1974.
- [18] H. Feshbach, A. Gal, and J. Hufner "On high-energy scattering by nuclei—II" *Ann. Phys.* vol. 66, 20-59, 1971.
- [19] T. de Forest and J.D Walecka "Electron Scattering and Nuclear Structure" *Adv. Phys.* vol. 15, no. 1, 1966.
- [20] B.A. Brown, R. A. Radhi and B.H. Wildenthal "Electric Quadrupole and Hexadecupole Nuclear Excitations from the Perspectives of Electron Scattering and Modern Shell-Model Theory" *Phys. Rep.* 101, no. 5, pp. 313-358. 1983.
- [21] A. G. Sitenko and V. K. Taratakovskii; "*Lectures on the theory of the Nucleus*"; (Pergamon press, Oxford, 1975.
- [22] B. A. Brown, A. Etchegoyen, N. S. Godwin, W. D. M. Rae, W. A. Richter, W. E. Ormand, E. K. Warburton, J. S. Winfield, L. Zhao and C. H. Zimmerman, *MSU-NSCL report number 1289*, 2005.
- [23] N. J. Stone, Table of nuclear magnetic dipole and electric quadrupole moments, International Data Committee, International Atomic Energy Agency (IAEA), INDC (NDS), 0658, 2014. B. A. Brown, A. Arima; and J. B. McGroory; *Nucl. Phys. A*, vol. 277, 77, 1977.
- [24] H. Sagawa and B. A. Brown "E2 Core Polrization for sd Shell Single-Particle States calculated with Skyrme-Type Interaction" *Nucl. Phys. A*, vol. 430, 84-98, 1984.
- [25] M. Carchidi, B. H. Wildenthal and B. A. Brown "Quadrupole moments of sd-shell nuclei" *Phys. Rev. C*, vol. 34, 2290, 1986.
- [26] A. Bohr and B. R. Mottelson; "*Nuclear Structure*", Benjamin, New York, 2, P. 515, 1975.
- [27] Yu. P. Gangrsky, D.V. Karaivanov, K.P. Marinova, B.N. Markov, L.M. Melnikova, G.V. Mishinsky, S.G. Zemlyanoi, V.I. Zhemelik "Hyperfine Splitting and Isotope Shift in the Atomic D2 Line of ^{22}Na , ^{23}Na and the Quadrupole Moment of ^{22}Na " *Eur. Phys. J. A*, vol. 3, 313-318, 1998.
- [28] K. Minamisono, K. Matsuta, T. Minamisono, C.D. P. Levy, T. Nagatomo, M. Ogura, T. Sumikama, J.A. Behr, K.P. Jackson, M. Mihara, M. Fukuda "Quadrupole moments of neutron-deficient $^{20,21}\text{Na}$ " *Phys. Lett. B*, vol. 672, 120–125, 2009.